



Article

Regression Analysis of Rectal Cancer and Possible Application of Artificial Intelligence (AI) Utilization in Radiotherapy

Majdi Alnowami ¹, Fouad Abolaban ^{1,2,*}, Hussam Hijazi ³ and Andrew Nisbet ⁴

- ¹ Department of Nuclear Engineering, Faculty of Engineering, King Abdulaziz University, P.O. Box 80204, Jeddah 21589, Saudi Arabia; malnowaimi@kau.edu.sa
- ² K. A. CARE Energy Research and Innovation Center, King Abdulaziz University, Jeddah 21589, Saudi Arabia
- ³ Radiation Oncology Unit, Radiology Department, Faculty of Medicine, King Abdulaziz University, P.O. Box 80204, Jeddah 21589, Saudi Arabia; hahijazi@kau.edu.sa
- ⁴ Department of Medical Physics & Biomedical Engineering, University College London, Malet Place Engineering Building, London WC1E 6BT, UK; andrew.nisbet@ucl.ac.uk
- * Correspondence: fabolaban@kau.edu.sa; Tel.: +966-503640153

Abstract: Artificial Intelligence (AI) has been widely employed in the medical field in recent years in such areas as image segmentation, medical image registration, and computer-aided detection. This study explores one application of using AI in adaptive radiation therapy treatment planning by predicting the tumor volume reduction rate (TVRR). Cone beam computed tomography (CBCT) scans of twenty rectal cancer patients were collected to observe the change in tumor volume over the course of a standard five-week radiotherapy treatment. In addition to treatment volume, patient data including patient age, gender, weight, number of treatment fractions, and dose per fraction were also collected. Application of a stepwise regression model showed that age, dose per fraction and weight were the best predictors for tumor volume reduction rate.



Citation: Alnowami, M.; Abolaban, F.; Hijazi, H.; Nisbet, A. Regression Analysis of Rectal Cancer and Possible Application of Artificial Intelligence (AI) Utilization in Radiotherapy. *Appl. Sci.* **2022**, *12*, 725. <https://doi.org/10.3390/app12020725>

Academic Editor: Qi-Huang Zheng

Received: 22 July 2021

Accepted: 3 September 2021

Published: 12 January 2022

Publisher's Note: MDPI stays neutral with regard to jurisdictional claims in published maps and institutional affiliations.



Copyright: © 2022 by the authors. Licensee MDPI, Basel, Switzerland. This article is an open access article distributed under the terms and conditions of the Creative Commons Attribution (CC BY) license (<https://creativecommons.org/licenses/by/4.0/>).

Keywords: radiotherapy; treatment planning; Artificial Intelligence; and tumor regression

1. Introduction

Approximately 50% of all cancer patients are treated using radiotherapy, with approximately 40% of patients who receive curative treatment for cancer being within this figure [1]. A patient's post diagnosis radiotherapy pathway may be considered to pass through several stages including pre-treatment imaging, treatment planning (TP), simulation, radiotherapy accessory production, radiotherapy verification, radiation delivery, and patient monitoring [2]. Clinicians depend on the information extracted from the images taken prior to and during treatment to develop an appropriate treatment plan that may be adapted to anatomical changes during treatment. Therefore, enhanced imaging modalities resulting in more precise data may make the therapy more efficacious. Previously, technological advances have enabled clinicians to model the delivered radiation fields to the tumor shape and have led to advanced treatments, such as intensity modulated radiation therapy (IMRT) and volumetric modulated arc radiotherapy (VMAT) [3]. In this era, further software and technology developments allow rapid and consistent production of automated treatment planning [4]. There are many classifications of automated treatment planning, such as knowledge-based, expert-based, or AI based treatment planning [5]. An oncologist can look at approximately 2400 treatment planning cases in 10 years, while AI can start with 2400 treatment planning cases to train itself and reach millions of cases within a concise period of time [6]. AI, and more specifically machine learning, has also been proposed as a tool to increase automation and optimization of workflows in radiotherapy [7–9]. By implementing the concept of AI to interrogate the tremendous amount of treatment data and medical images available at any hospital, one may enable the delivery of improved stratified or personalized treatment [10,11].

Information that may help with accurate decisions on radiation therapy treatment planning include a patient's tumor mass, height, weight, body mass index and previous exposure to radiation. Together with internal medical images of the patient that are obtained and analyzed, one may personalize the therapy by modifying different treatment planning parameters. AI has already been employed broadly in recent years in the medical field including data mining and knowledge discovery in medicine, medical expert systems, machine learning-based medical systems, and medical signal and image processing techniques [6,12,13]. Researchers have also demonstrated promising progress and a future for AI to be widely used in medical imaging, image segmentation, medical image registration, computer-aided detection (CAD) and diagnosis systems, as well as in treatment planning [5,14,15].

The radiotherapy treatment planning (TP) primary goal is reducing radiation dose to surrounding organs-at-risk (OAR) while maximizing dose to the tumor or target volume. This can be achieved by collecting accurate information about the tumor and the selected treatment, such as beam intensity shaping, planning margin, calculation of organ motion, therapy technique selection, and optimization of treatment planning [14]. An initial radiation treatment plan may not suit a patient well throughout the entire course of treatment due to, for example, post-surgical oedema, weight loss, or a change in tumor size or shape. Therefore, an adaptive plan may be created by acquiring a new set of images at some point over the treatment course and applying new parameters, e.g., new volumes or different prescription dose levels, for the remainder of the treatment. This process is called adaptive radiotherapy (ART). The need for quality assurance and methodical implementation of AI in clinical practice has been highlighted [16]. Furthermore, ART has yet to be fully implemented in clinical practice with questions still remaining on optimum practices, including when imaging should be undertaken to help with identification of patients requiring adaptive treatment plans [17,18]. This study therefore investigates the possibility of using AI in adaptive radiation therapy (ART). Complete treatment information for 20 rectal cancer cases was obtained from King Abdulaziz University Hospital to attempt using AI in determining the rate of target volume change during the treatment. This may lead to a better understanding of the implementation of one application of Artificial Intelligence in adaptive radiotherapy treatment planning.

2. Materials and Methods

2.1. Tumour Site Delineation and Contouring

Twenty randomly selected patients with rectal cancer treated at King Abdulaziz University Hospital, a specialist radiation oncology unit, were identified using a commercially available record and verification system, Mosaic[®] (Elekta AB, Sweden).

The patients mainly received a total dose of 45 Gy or 50 Gy in 25 or 28 fractions respectively of 1.8 or 2 Gy per fraction (RCR 2021). Inclusion criteria:

- Aged 18–80 years old;
- Locally advanced adenocarcinoma of the rectum;
- Received neoadjuvant long course chemo-radiotherapy;
- Treated with Elekta LINAC machines using the Monaco treatment planning system;
- Daily CBCT was performed for image verification throughout the whole treatment course.

Full details on each respective patient including variations on this fractionation regimen are tabulated in Table 1. Five Cone Beam Computed Tomography (CBCT) Scans were obtained for each patient, one CBCT per week for the entire five weeks of the treatment course. CBCTs were then transferred to a commercially available Treatment Planning System, Monaco[®] (Elekta AB, Sweden) for contouring. Rectal contours were delineated on each CBCT after image registration with a pre-treatment CT planning scan to obtain the volume of the rectum over the treatment course.

Approximately 100 rectal volume values from CBCTs were used in the analysis in addition to the rectal volumes of CT planning contours. The CBCT taken in the first week

of treatment was used as the reference image. Such sample numbers are in line with other similar reported studies on AI in radiotherapy [19].

Table 1. Patient data collected from King Abdulaziz University Hospital, Radiotherapy Department.

Patient	GTV (cm ³)	CBCT Week 1 (cm ³)	CBCT Week 2 (cm ³)	CBCT Week 3 (cm ³)	CBCT Week 4 (cm ³)	CBCT Week 5 (cm ³)	Total Dose Gy	Patient Age (Years)	Patient Gender	No. of Treatment Fractions	Dose per Fraction (Gy)	Patient Weight (Kg)
Patient 1	89.9	87.07	74.97	49.35	55.3	64.79	50	71	Female	28	1.8	45
Patient 2	47.6	48.62	39.39	40.37	40.65	40.46	50	60	Male	25	2	84
Patient 3	57.21	51.498	43.099	40.199	40.698	45.188	50	58	Female	28	1.8	87
Patient 4	41.42	34.157	37.807	35.105	35.437	31.321	50	45	Female	28	1.8	69
Patient 5	90.66	89.871	93.785	92.89	90.643	87.908	50	53	Female	28	1.8	50
Patient 6	227	223.9	225.35	224.77	228.54	227.98	50	50	Male	28	1.8	77
Patient 7	40.86	36.986	38.564	37.654	39.876	34.874	50	67	Female	25	2	70
Patient 8	68.03	61.985	63.986	64.963	67.734	67.097	50	50	Male	28	1.8	-
Patient 9	105	102.95	101.79	104.88	106.78	102.65	50	74	Male	25	2	-
Patient 10	51.86	35.482	36.725	38.125	40.228	31.245	50	75	Male	28	1.8	60
Patient 11	32.06	46.151	33.645	37.559	44.052	38.312	50	56	Male	25	2	72
Patient 12	47.45	38.38	42.522	45.725	41.711	48.162	50	56	Male	28	1.8	-
Patient 13	35.9	34.486	32.686	33.512	28.759	29.051	59	59	Male	33	1.8	50
Patient 14	67.48	86.735	82.028	103	96.808	96.375	45	39	Female	25	1.8	-
Patient 15	89.92	78.076	74.978	68.008	65.305	64.289	45	71	Female	25	1.8	42
Patient 16	68.87	67.142	57.852	88.589	57.852	57.895	50	37	Male	25	1.8	60
Patient 17	64.85	63.481	53.649	61.882	54.191	51.232	50	59	Male	28	1.8	76
Patient 18	74.34	69.04	42.188	43.357	29.12	32.043	50	68	Male	28	1.8	83
Patient 19	56.46	61.975	59.67	55.891	58.569	60.864	45	38	Female	25	1.8	56
Patient 20	74.98	80.324	78.983	77.973	73.848	74.868	50	71	Male	25	2	88

2.2. Intra-Treatment Rectum Tumor Volume Change

The tumor target volume was defined on the prior planning CT and for all treatment CT images, and three-dimensional tumor volumes were calculated on the planning system as per RECIST v.1.1 [20]. Changes in the gross tumor volume (GTV) between the CT images were analyzed. Rectal volume change rate was defined as the percentage (%) reduction of the GTV in relation to the pre-RT GTV, where:

$$\text{Rectal volume change rate} = \frac{(V_0 - V_t)}{V_0} \times 100 \quad (1)$$

where V_0 is the pre-RT gross tumor volume, t represents time, and V_t the post-RT Gross Tumor Volume. Table 2 demonstrates the volume change rate of the 20 patients included in this study. Patients had a median age of 57 (range 37–75) years. The mean pre-RT tumor volume was $71.6 \pm 40.7 \text{ cm}^3$, and the mean post-RT tumor volume was $64.3 \pm 43.2 \text{ cm}^3$. As illustrated in Table 2, the mean tumor volume reduction rate (TVRR) of 10.9 % (range, 56.9 to –42.8) was calculated according to equation 1. Four patients resulted in a negative TVRR with their tumor volumes appearing enlarged after radiotherapy. There may be a number of possible explanations for this. This may be due to different levels of rectal filling throughout the treatment course on the assumption the surface area of the delineated tumor is increased when the rectum is distended due to fecal material or gas. This is common despite patients' instructions regarding bowel preparation before each radiotherapy session. Some patients fail to follow these instructions or may suffer from chronic constipation or other co-morbidities. However, it may relate to actual tumor growth or proliferation, an inflammatory response to treatment, tissue swelling, or uncertainties in contouring, further investigation of this is required.

Table 2. Tumor volume change for all patients.

Patient	Total Dose Gy	Age (Years)	Gender	No. of Treatment Fractions	Dose per Fraction (Gy)	Weight (kg)	Volume Change %
Patient 1	50.4	71	Female	28	1.8	45	27.93
Patient 2	50	60	Male	25	2	84	15
Patient 3	50.4	58	Female	28	1.8	87	21.02
Patient 4	50.4	45	Female	28	1.8	69	24.38
Patient 5	50.4	53	Female	28	1.8	50	3.03
Patient 6	50.4	50	Male	28	1.8	77	−0.43
Patient 7	50	67	Female	25	2	70	14.65
Patient 8	50.4	50	Male	28	1.8	-	1.37
Patient 9	50	74	Male	25	2	-	2.23
Patient 10	50.4	75	Male	28	1.8	60	39.75
Patient 11	50	56	Male	25	2	72	−19.5
Patient 12	50.4	56	Male	28	1.8	-	−1.51
Patient 13	59.4	59	Male	33	1.8	50	19.07
Patient 14	45	39	Female	25	1.8	-	−42.81
Patient 15	45	71	Female	25	1.8	42	28.5
Patient 16	50.4	37	Male	25	1.8	60	15.94
Patient 17	50.4	59	Male	28	1.8	76	20.99
Patient 18	50.4	68	Male	28	1.8	83	56.9
Patient 19	45	38	Female	25	1.8	56	−7.81
Patient 20	50	71	Male	25	2	88	0.15

2.3. Relation between TVRR and a Patient's Clinical Variables

The relation between the target volume reduction rate and a patient's clinical variables such as age, total dose (Gy), gender, number of treatment fractions, dose per fraction, and patient weight was analyzed. Tables 1 and 2 record the different variables in the patient dataset. Thus, the range of the variables may differ substantially between patients. Hence, using the original scale will by default apply more weight on the variables with an extensive range. Therefore, feature rescaling to independent variables or features of data, in data pre-processing were applied. The purpose of employing feature rescaling is to ensure a patient's different clinical variables are on almost the same scale, in order that each variable is equally weighted in importance. The standardization outcome is that the variables will be rescaled to ensure the mean and the standard deviation are 0 and 1, respectively.

$$D_s = (D - D_m) / D_{std} \quad (2)$$

where D is the original data, D_s the scaled data, and D_m and D_{std} the mean and standard deviation of each variable, respectively.

The significance of each patient's clinical variable was examined independently using a statistical F-test. These were based on the hypothesis that the variable values put together with the tumor volume reduction rate (TVRR) values are drawn from populations with the same mean, against the alternative hypothesis that the population means are not all the same. A small p -value of the test statistic implies that the corresponding variable is essential. The output score is $-\log(p)$. Therefore, a considerable score value indicates that the corresponding variable is important. The mixture technique used in this study relies on defining the Nano-particles (NPs) as a mixture with its parent volume (the volume the NPs are embedded within). This technique was reported to overestimate the dose in some

cases [21], but is faster to compute, easier to implement, and is useful when the objective is to compare different types of NPs and provide a general understanding of their effect on dosimetric quantities. The major drawback of this technique is that it does not allow studying the size or shape of the NPs, which is out of this study's scope.

2.4. Data Analysis

Stepwise regression is a method that iteratively examines each independent variable's statistical significance in a linear regression model. The underlying goal of stepwise regression is, through a series of tests (F-tests, *t*-tests), to find a set of independent variables that significantly influence the dependent variable.

In statistics, the *p*-value is the probability of obtaining results at least as the observed results of a statistical hypothesis test, assuming that the null hypothesis is correct. The *p*-value is used as an alternative to rejection points to provide the smallest level of significance at which the null hypothesis would be rejected. A smaller *p*-value means that there is more substantial evidence in favor of the alternative hypothesis. We then examine how well a linear regression model fits the data using the selected variables.

3. Results

Figure 1 shows a bar plot of the patients' clinical variables importance score. The figure shows that dose per fraction and weight have a higher correlation with tumor volume change than other clinical variables. However, this bar plot does not reflect the relationship between variables and whether any combination of variables may have a higher correlation with the volume change.

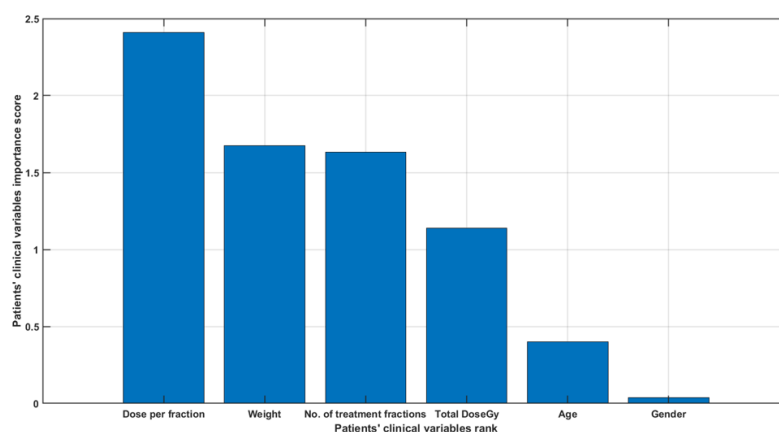


Figure 1. A bar plot of the patients' clinical variables importance score.

Partial dependence plot (PDP) and individual conditional expectation (ICE) analysis: partial dependence plots (PDP) and individual conditional expectation (ICE) plots, as seen in Figure 2, can be used to visualize and analyze the interaction between the tumor volume reduction rate and a set of input predictors. The partial dependency map (also known as the PDP or PD plot) illustrates the marginal effect of one or two features on the predicted outcome of a machine learning algorithm. A partial dependency plot can demonstrate whether the relationship between a percentage volume change and variable is linear, monotonic, or more complex. Individual conditional expectation (ICE) plots demonstrate how the prediction of an instance varies when an attribute changes. Since it focuses on a general average rather than particular cases, the partial dependency plot for the average influence of a feature is a global technique. Figure 2 plots the corresponding PD line in red overlaid on ICE lines in grey. A scatter plot of the selected predictor and predicted responses is also included for all patients. The figure shows that gender, number of treatment fractions and dose per fraction do not affect volume change within the patient group studied. However, dose per fraction, age, and weight appear to correlate with percentage volume change within this patient group.

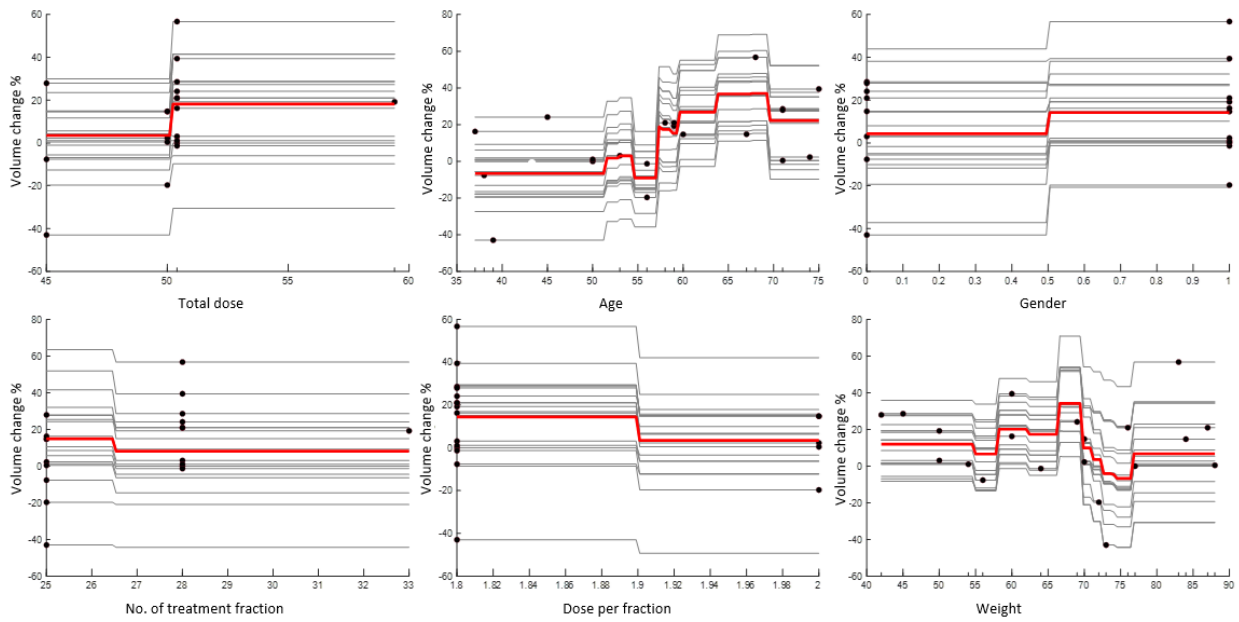


Figure 2. A PDP plot (red line) and ICE plots (grey lines) for each predictor. A scatter plot (circle markers) of the selected predictor and predicted responses is also included.

While PDPs figures are useful for displaying the average influence of the individual target features, they may mask a connection caused by interactions between target features. Figure 3 visualizes the partial dependence of predicted responses (percentage volume change) on the predictor variables dose per fraction and age. The figure shows that the volume change % was at its lowest range at a younger age and higher dose per fraction. Figure 4 visualizes the partial dependence of predicted responses (percentage volume change) on the predictor variables weight and age. Figure 5 shows the partial dependence of predicted responses (percentage volume change) on the predictor variables' dose per fraction and weight. Figure 4 again reflects the positive impact of the younger age and lower weight. Figures 3–5 show that younger age and low weight with a higher dose per fraction reflect better treatment outcome in terms of the volume change %, further investigation of this is required.

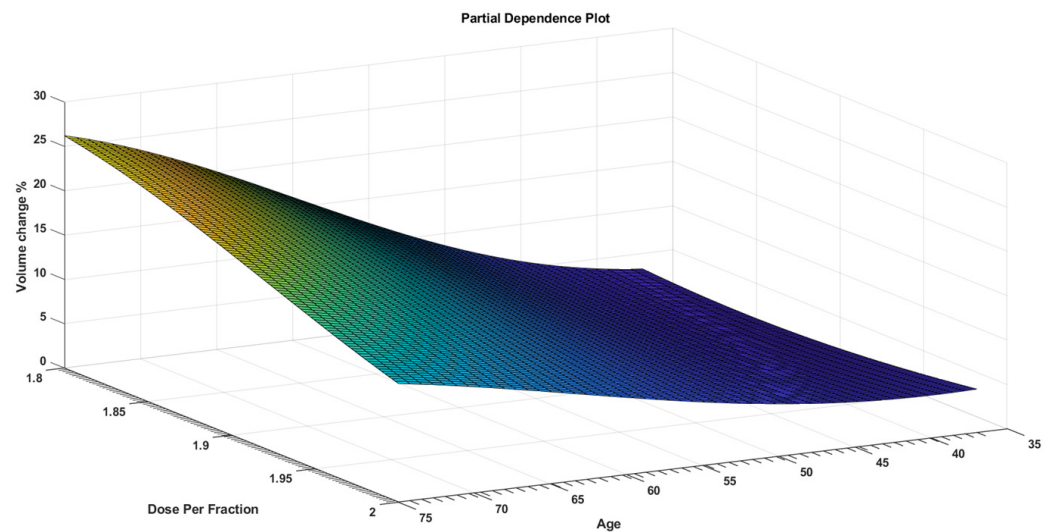


Figure 3. A PDP that visualizes partial dependence of predicted responses (volume change %) on the predictor variables dose per fraction and age.

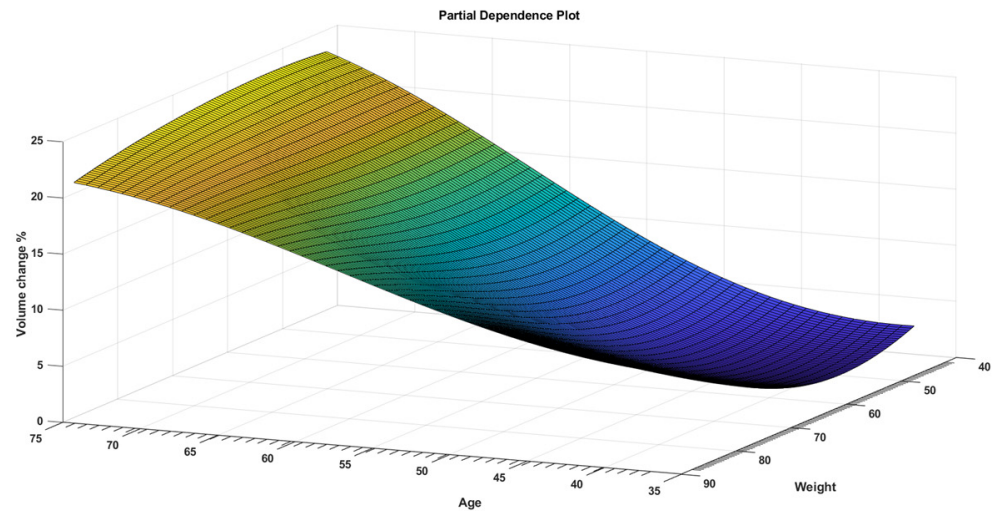


Figure 4. A PDP that visualizes partial dependence of predicted responses (volume change %) on the predictor variables weight and age.

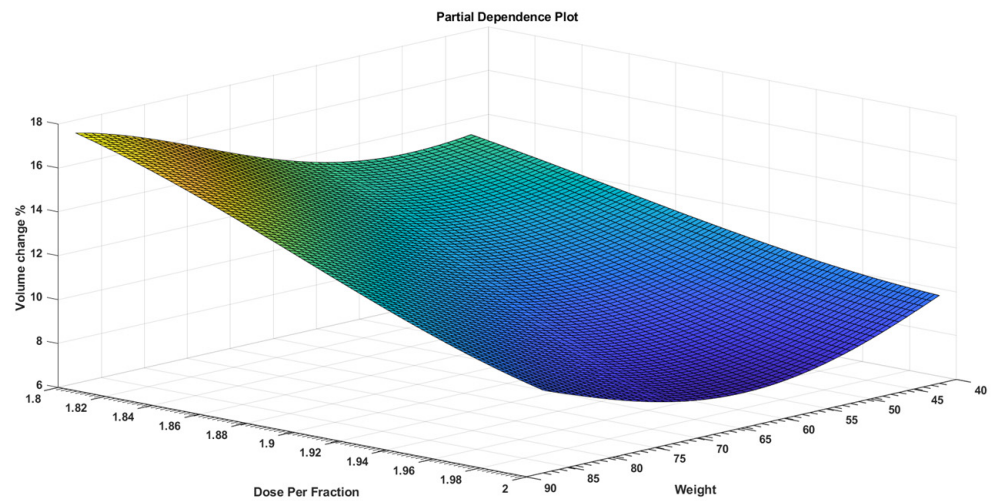


Figure 5. A PDP that visualizes partial dependence of predicted responses (volume change %) on the predictor variables dose per fraction and weight.

The result shown in Table 3 demonstrate that age provides the main interest after the first iteration. In the next step additional predictors are added to age and the p -value of each additional predictor calculated again. The steps described above are repeated until adding an additional predictor does not yield a better t -test and p -value. The stepwise regression model showed that age, dose per fraction and weight are best predictors for tumour volume reduction rate and the relationship can be summarized in the following equation, where c_1 , c_2 , and c_3 are constants:

$$\text{TVRR} \sim 1 + c_1 \text{ Age} + c_2 \text{ Dose Per Fraction} + c_3 \text{ Weight} \quad (3)$$

Using the result obtained one may fit a stepwise linear regression model to the data to determine how well the model fits the data. The root mean squared error (RMSE) of the linear regression is 0.164. Table 4 tabulates the goodness-of-fit statistics.

Table 3. Artificial Intelligence coding iteration.

Iteration 1			Iteration 2		Iteration 3	
Patients' clinical variables	Total Dose	<i>p</i> Value 0.169	Total Dose + Age	0.282	Total Dose + Age + Dose Per Fraction	<i>p</i> Value 0.182
	Age	0.018				
	Gender	0.704	Gender + Age	0.985	Gender + Age + Dose Per Fraction	0.485
	No. of Treatment Fractions is	0.106	No. of Treatment Fractions + Age	0.089	No. of Treatment Fractions + Age + Dose Per Fraction	0.079
	Dose Per Fraction	0.326	Dose Per Fraction + Age	0.016		
	Weight	0.055	Weight + Age	0.064	Weight + Age + Dose Per Fraction	0.002

Table 4. Estimated coefficients used in AI coding.

	Estimate	SE	tStat	<i>p</i> Value
(Intercept)	180.5	64.253	2.8092	0.0126
Age	1.2172	0.27207	4.4737	0.000384
Dose Per Fraction	−138.86	37.271	−3.7256	0.00184
Weight	0.31647	0.10096	3.1345	0.006399

The accuracy of the model in predicting the tumor volume reduction rate is illustrated in Figure 6. This plots the TVRR as calculated by Equation (3) and the actual measured TVRR. Figure 7 provides an alternative representation of these results showing the difference between predicted TVRR and actual TVRR for each of the 20 patients.

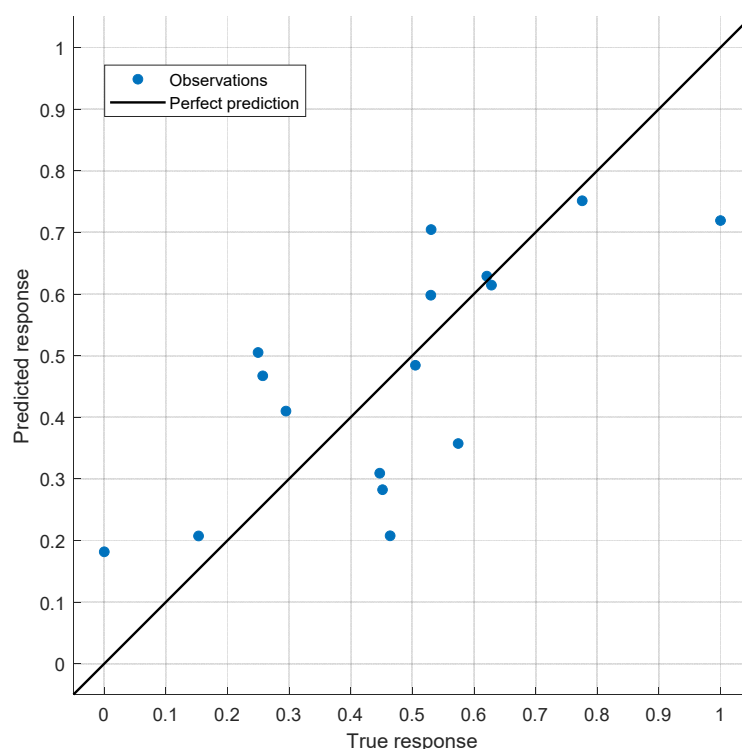


Figure 6. The predicted TVRR vs. the actual TVRR.

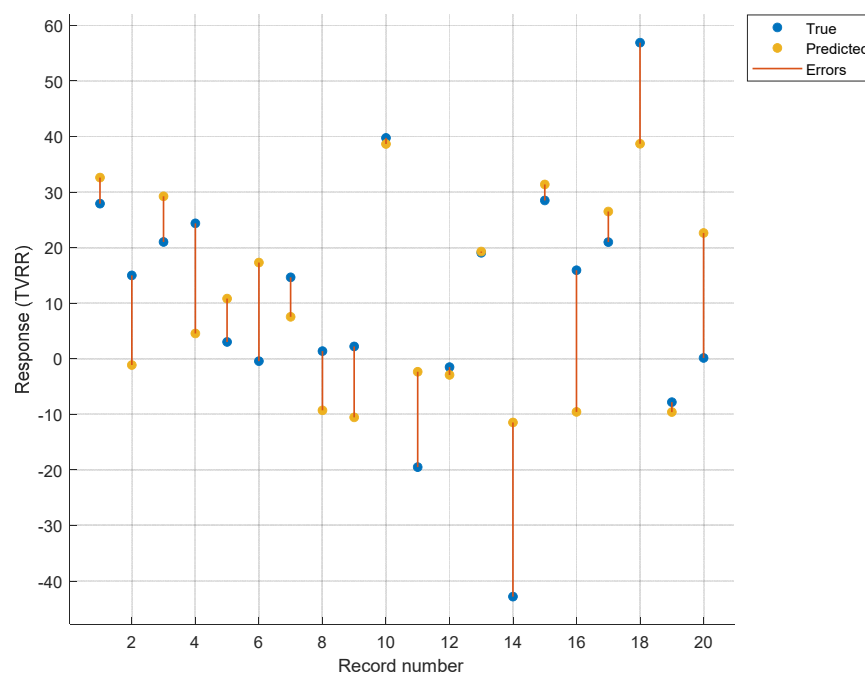


Figure 7. The predicted TVRR is plotted against the actual TVRR with individual differences shown in yellow.

4. Discussion

A number of studies have investigated tumor volume dynamics in response to radiotherapy. Tariq et al. (2015) employed a mathematical modelling approach including sufficient details of radiobiological theory to describe tumor volume dynamics in 18 non-small cell lung cancer (NSCLC) patients' response to stereotactic ablative radiotherapy (SABR). This work highlighted the significant variability of the estimated model parameters across different patients, suggesting that, if the model is intended to describe GTV dynamics for individual patients, then a population modelling approach may not be desired.

Further work considered starting with a population-average model subsequently updated from an individual's tumor volume change to develop a more personalized prediction, based on 25 NSCLC patients treated with helical tomotherapy [22]. Belfatto et al. considered a mathematical model of tumor response to radiotherapy based on CBCT data for 13 uterine cervical cancer patients, with promising results ranging from 13% to 21% for average model fitting errors on three group specific parameter sets based on tumor type and treatment and one general parameter set.

Such mathematical approaches are dependent to some extent on the ability of radiobiological models to accurately reflect a complex tumor microenvironment and its response to radiation and such models are largely population derived. The potential advantage of a more empirical AI based approach using individual patient characteristics is in a more personalized, or at least stratified, prediction. The AI approach described within this work presents promising results with a mean difference between predicted and actual volume change of $6.5\% \pm 2.5\%$, based on a stepwise regression model which demonstrated that age, dose per fraction and weight were the best predictors for TVRR.

The patient sample within this study is small, although of the order of previous studies, and hence it is to be expected that improved results may be obtained with a larger patient sample. For further validation of the model the results should ideally be tested with an independent dataset. However, this is a preliminary feasibility study and further development of the model with more patients is planned.

It is important to note that the results obtained within this study of rectal cancer patients will not be applicable to other cancer sites, although a similar methodology may be employed.

For some cancer sites it will also be important to consider changes in the volume of nearby organs at risk (OAR) in order to develop an effective adaptive radiotherapy strategy.

5. Conclusions

This study presents a case study demonstrating the feasibility of employing artificial intelligence in a cohort of rectal cancer patients for adaptive radiotherapy by predicting the tumor volume reduction rate (TVRR). Cone beam computed tomography (CBCT) scans of twenty rectal cancer patients were collected to observe the change in tumor volume over the course of a standard five-week radiotherapy treatment. Application of a stepwise regression model showed that age, dose per fraction and weight were the best predictors for TVRR with a mean difference between predicted and actual volume change of $6.5\% \pm 2.5\%$. Such an approach may be further developed to aid in the clinical implementation of adaptive radiotherapy.

Author Contributions: Conceptualization, F.A.; methodology, F.A. and M.A.; software, M.A.; validation, F.A. and M.A.; formal analysis, M.A. and H.H.; investigation, F.A. and H.H.; resources, F.A.; data curation, H.H.; writing—original draft preparation, F.A.; writing—review and editing, A.N.; visualization, F.A.; supervision, A.N.; project administration, F.A.; funding acquisition, F.A. All authors have read and agreed to the published version of the manuscript.

Funding: The Authors acknowledge the support provided by King Abdullah City for Atomic and Renewable Energy (K.A.CARE) under K.A.CARE-King Abdulaziz University Collaboration Program. The authors are also thankful to Deanship of Scientific Research, King Abdulaziz University for providing financial support vide grant number (RG-88-135-42).

Institutional Review Board Statement: This study was conducted retrospectively utilizing data gathered for clinical purposes. We collaborated closely with King Abdulaziz University Hospital Ethics Committee, which determined that our study did not require ethical approval. Because of the retrospective nature of the study and the fact that all of the operations were part of standard care, ethical approval was not required.

Informed Consent Statement: The research involves data that have been collected solely for non-research purposes (medical treatment or diagnosis). The data sources are publicly available and the subject cannot be identified directly or through identifiers linked to the subject.

Data Availability Statement: The authors confirm that the data supporting the findings of this study are available within the article.

Conflicts of Interest: The authors declare no conflict of interest.

References

1. Baskar, R.; Lee, K.A.; Yeo, R.; Yeoh, K.-W. Cancer and Radiation Therapy: Current Advances and Future Directions. *Int. J. Med. Sci.* **2012**, *9*, 193–199. [[CrossRef](#)] [[PubMed](#)]
2. Khoo, V.S. Radiotherapeutic techniques for prostate cancer, dose escalation and brachytherapy. *Clin. Oncol.* **2005**, *17*, 560–571. [[CrossRef](#)]
3. Teoh, M.; Clark, C.H.; Wood, K.; Whitaker, S.; Nisbet, A. Volumetric modulated arc therapy: A review of current literature and clinical use in practice. *Br. J. Radiol.* **2011**, *84*, 967–996. [[CrossRef](#)] [[PubMed](#)]
4. Hussein, M.; Heijmen, B.J.M.; Verellen, D.; Nisbet, A. Automation in intensity modulated radiotherapy treatment planning—a review of recent innovations. *Br. J. Radiol.* **2018**, *91*. [[CrossRef](#)] [[PubMed](#)]
5. Nwankwo, O.; Mekdash, H.; Sihono, D.S.K.; Wenz, F.; Glattig, G. Knowledge-based radiation therapy (KBRT) treatment planning versus planning by experts: Validation of a KBRT algorithm for prostate cancer treatment planning. *Radiat. Oncol.* **2015**, *10*, 111. [[CrossRef](#)]
6. Siddique, S.; Chow, J.C.L. Artificial intelligence in radiotherapy. *Rep. Pract. Oncol. Radiother.* **2020**, *25*, 656–666. [[CrossRef](#)]
7. DJarrett, D.; Stride, E.; Vallis, K.; Gooding, M.J. Applications and limitations of machine learning in radiation oncology. *Br. J. Radiol.* **2019**, *92*. [[CrossRef](#)]
8. El Naqa, I.; Ruan, D.; Valdes, G.; Dekker, A.; McNutt, T.; Ge, Y.; Wu, Q.J.; Oh, J.H.; Thor, M.; Smith, W.; et al. Machine learning and modeling: Data, validation, communication challenges. *Med. Phys.* **2018**, *45*, e834–e840. [[CrossRef](#)] [[PubMed](#)]
9. Feng, M.; Valdes, G.; Dixit, N.; Solberg, T.D. Machine Learning in Radiation Oncology: Opportunities, Requirements, and Needs. *Front. Oncol.* **2018**, *8*, 110. [[CrossRef](#)]

10. Lustberg, T.; van Soest, J.; Jochems, A.; Deist, T.; van Wijk, Y.; Walsh, S.; Lambin, P.; Dekker, A. Big Data in radiation therapy: Challenges and opportunities. *Br. J. Radiol.* **2017**, *90*. [[CrossRef](#)]
11. Huynh, E.; Hosny, A.; Guthier, C.; Bitterman, D.S.; Petit, S.F.; Haas-Kogan, D.A.; Kann, B.; Aerts, H.J.; Mak, R.H. Artificial intelligence in radiation oncology. *Nat. Rev. Clin. Oncol.* **2020**, *17*, 771–781. [[CrossRef](#)]
12. Chan, Y.K.; Chen, Y.F.; Pham, T.; Chang, W.; Hsieh, M.Y. Artificial Intelligence in Medical Applications. *J. Healthc. Eng.* **2018**, *2018*. [[CrossRef](#)] [[PubMed](#)]
13. Wang, C.; Zhu, X.; Hong, J.-C.; Zheng, D. Artificial Intelligence in Radiotherapy Treatment Planning: Present and Future. *Technol. Cancer Res. Treat.* **2019**, *18*, 153303381987392. [[CrossRef](#)] [[PubMed](#)]
14. van de Bunt, L.; van der Heide, U.A.; Ketelaars, M.; de Kort, G.A.P.; Jürgenliemk-Schulz, I.M. Conventional, conformal, and intensity-modulated radiation therapy treatment planning of external beam radiotherapy for cervical cancer: The impact of tumor regression. *Int. J. Radiat. Oncol. Biol. Phys.* **2006**, *64*, 189–196. [[CrossRef](#)]
15. Miras, H.; Jiménez, R.; Perales, Á.; Terrón, J.A.; Bertolet, A.; Ortiz, A.; Macías, J. Monte Carlo verification of radiotherapy treatments with CloudMC. *Radiat. Oncol.* **2018**, *13*, 99. [[CrossRef](#)] [[PubMed](#)]
16. Liesbeth, V.; Michaël, C.; Anna, M.D.; Charlotte, L.B.; Wouter, C.; Dirk, V. Overview of artificial intelligence-based applications in radiotherapy: Recommendations for implementation and quality assurance. *Radiother. Oncol.* **2020**, *153*, 55–66. [[CrossRef](#)]
17. Brouwer, C.L.; Steenbakkers, R.J.H.M.; Langendijk, J.A.; Sijtsema, N.M. Identifying patients who may benefit from adaptive radiotherapy: Does the literature on anatomic and dosimetric changes in head and neck organs at risk during radiotherapy provide information to help? *Radiother. Oncol.* **2015**, *115*, 285–294. [[CrossRef](#)]
18. LEE, V.S.-C.; SchettIno, G.; Nisbet, A. UK adaptive radiotherapy practices for head and neck cancer patients. *BJROpen* **2020**, *2*, 20200051. [[CrossRef](#)] [[PubMed](#)]
19. Humbert-Vidan, L.; Patel, V.; Oksuz, I.; King, A.P.; Guerrero Urbano, T. Comparison of machine learning methods for prediction of osteoradionecrosis incidence in patients with head and neck cancer. *Br. J. Radiol.* **2021**, *94*, 20200026. [[CrossRef](#)]
20. Eisenhauer, E.A.; Therasse, P.; Bogaerts, J.; Schwartz, L.H.; Sargent, D.; Ford, R.; Dancey, J.; Arbuck, S.; Gwyther, S.; Mooney, M.; et al. New response evaluation criteria in solid tumours: Revised RECIST guideline (version 1.1). *Eur. J. Cancer* **2009**, *45*, 228–247. [[CrossRef](#)] [[PubMed](#)]
21. Zhang, S.-X.; Gao, J.; Buchholz, T.A.; Wang, Z.; Salehpour, M.R.; Drezek, R.A.; Yu, T.-K. Quantifying tumor-selective radiation dose enhancements using gold nanoparticles: A monte carlo simulation study. *Biomed. Microdevices* **2009**, *11*, 925–933. [[CrossRef](#)] [[PubMed](#)]
22. Tariq, I.; Humbert-Vidan, L.; Chen, T.; South, C.P.; Ezhil, V.; Kirkby, N.F.; Jena, R.; Nisbet, A. Mathematical modelling of tumour volume dynamics in response to stereotactic ablative radiotherapy for non-small cell lung cancer. *Phys. Med. Biol.* **2015**, *60*, 3695–3713. [[CrossRef](#)] [[PubMed](#)]